Available online at www.sciencedirect.com
ScienceDirect
Trans. Nonferrous Met. Soc. China 26(2016) 1269−1275
Transactions of Nonferrous Metals Society of China
www.tnmsc.cn

Interface analysis of 7B52 Al alloy laminated composite fabricated by hot-roll bonding

Gu-xin ZHOU, Yu-jing LANG, Jie HAO, Wen LIU, Sheng WANG, Li QIAO, Min CHEN

Ningbo Branch of China Academy of Ordnance Science, Ningbo 315103, China

Received 12 May 2015; accepted 24 February 2016

Abstract: The bonding interface of 7B52 Al alloy laminated composite (ALC) fabricated by hot rolling was investigated using optical microscopy (OM), transmission electron microscopy (TEM), scanning electron microscopy (SEM), ultrasonic flaw detection (UFD), and bonding strength tests. The results show that metallurgical bonding is achieved at the interface after composite rolling. The TEM analysis and tensile tests indicate that the 7B52 ALC plate combines high strength of the hard individual layer and good toughness of the soft individual layer. However, UFD technology and SEM analysis prove that the defects (thick oxide films, acid washed residues, air, oil and coarse particles) existing in the bonding interface are harmful to the bonding strength. To sum up, the composite rolling process is suitable for 7B52 ALC plate, and the content and size of the defects should be controlled strictly. Advanced surface treatment of each individual layer would be beneficial to further improve the bonding quality.

Key words: 7B52 aluminium alloy laminated composite; hot-roll bonding; microstructure; interfacial analysis

1 Introduction

Al alloys are essential structural materials for vehicle, aviation, marine and power generation systems as a means of weight reduction [1,2], and the demand of these alloys keeps increasing in modern industry. However, a single alloy does not always satisfy the strict requirements for special application. High-performance composite materials with special structures and functions are considered as the ideal approaches.

As one of the most important composite materials, laminated composite metals consisted of two or more metal alloys with different properties can be manufactured by special manufacturing processes [3−7]. Specifically, Al laminated composites (ALCs) with combined high strength and good toughness have been successfully designed by reasonably bonding distinct Al alloys with higher strength or higher ductility [8−14]. They have the excellent particular performances, such as ballistic protection, blast mitigation, thermal management, heat exchange and vibration damping [15]. The projectile-resistance property of 7B52 ALC plate has been improved by 10%−15%, compared with that of 7A52 Al homogenous plate [16].

The ultrasonic flaw detection (UFD) technology has been used in extensively industrial applications (aeronautical materials testing, welding seam organization, pressure vessel, petroleum pipelines and automotive engines [17]) due to the great demand for non-destructive testing (NDT), which is an effective measurement to evaluate the manufacturing quality and operation integrity of those structures and systems [18]. Here, we explore the interface bonding of the 7B52 laminated plate by UFD.

The goals of this work are to investigate the bonding interface and the interfacial strength of the laminated plate and thus to evaluate the manufacturing quality of the 7B52 ALC plate. UFD method was used to characterize the bonding interface and analyze the factors generating interface flaw thoroughly, which will provide guideline for optimizing composite rolling process.

2 Experimental

Triple ingots of Al−Zn−Mg, Al−Zn and Al−Zn−

Foundation item: Project (51312JQ08) supported by the Pre-Research Foundation of China General Equipment Department; Project (NBPJ2013-4) supported by the Postdoctoral Science Foundation of Ningbo Branch of China Academy of Ordnance Science; Project (bsh1402073) supported by the Postdoctoral Science Foundation of Zhejiang Province, China; Project (2014A610051) supported by the Ningbo Natural Science Foundation of China

Corresponding author: Yu-jing LANG; Tel: +86-574-87902209; Fax: +86-574-87902208; E-mail: yj.lang@163.com

DOI: 10.1016/S1003-6326(16)64227-9

Mg−Cu alloys were homogenized at 470 °C for 24 h with subsequent air cooling. After surface treatment by acid washing, the triple homogenized ingots were hot rolled and deformed into a composite plate. This composite plate is defined as 7B52 Al alloy. Next, the plate was solution treated at 470 °C for 2 h with immediate quenching in water at room temperature and artificially aged at 120 °C for 24 h (T6 treatment). Finally, the 7B52 ALC plate with the dimensions of 60 mm × 100 mm × 400 mm was obtained.

Microstructure of 7B52 ALC plate was examined by optical microscopy (OM, LEICA MEF4M) and transmission electron microscopy (TEM, FEI TECNAI G2), and the bonding interface of the alloy was observed using scanning electron microscopy (SEM, QUANTA FEG250) equipped with energy dispersive spectroscopy (EDS). The specimens for OM and SEM observation were prepared by standard metallographic procedures using Keller's reagent. The thin foils for TEM observation were prepared by twinjet electro-polishing in the solution of 70% methanol and 30% nitric acid at −20 °C. The flaws of bonding interface of 7B52 ALC plate were studied using ultrasonic flaw detection C-SCAN system, which was based on conducting and propagating ultrasound waves, generated by a transducer, through the structural materials. Then, when there is a flaw in the wave path, part of its energy will be reflected back from the flaw surface and transformed into C scan data acquisition and imaging. Mechanical property tests and bonding strength tests were carried out on a CMT−4105 test machine at room temperature with a nominal strain rate of 1×10^{-3} s^{-1}.

3 Results

3.1 Microstructure

Analyzing the structure and interface characteristics of individual layer of the 7B52-T6 ALC plate is the premise and foundation of establishing the relationship of mechanical properties. Obviously, Fig. 1 shows a good metallurgical bonding without micro-cracks between three Al alloys (Al−Zn−Mg alloy/Al−Zn alloy/Al−Zn−Mg−Cu alloy) which was attained by the roll bonding and heat treatment. Besides the Al−Zn−Mg and Al−Zn−Mg−Cu alloys composed of the elongated grains, two visibly straight interfaces were obtained by composition design and matching thickness. The straight interfaces are different from the visible warped interfaces of 1100/7075 laminated composite sheets reported by CHEN et al [14]. The shape of these interfaces depends on the hot-roll bonding process. Figure 1 also shows that some insoluble second particles, such as *S* (Al_2CuMg) phase and Fe-rich (Al_7Cu_2Fe) phase exist in Al−Zn−Mg−Cu alloy, but *T* ($Al_2Mg_3Zn_3$) phase and Fe-rich phase exist in Al−Zn−Mg alloy. The mechanical properties of the 7B52-T6 ALC plate will depend on both the individual layer and the bonding interfaces.

Figure 2 shows the TEM images of Al−Zn−Mg alloy and Al−Zn−Mg−Cu alloy in the 7B52-T6 ALC plate. A large number of nano-scaled particles precipitate from the matrix, which mainly induce the precipitation hardening during artificial aging for Al−Zn−Mg alloy and Al−Zn−Mg−Cu alloy. The size of the nano-scaled particles and the distance between particles in the Al−Zn−Mg alloy (Fig. 2(a)) are slightly larger than those

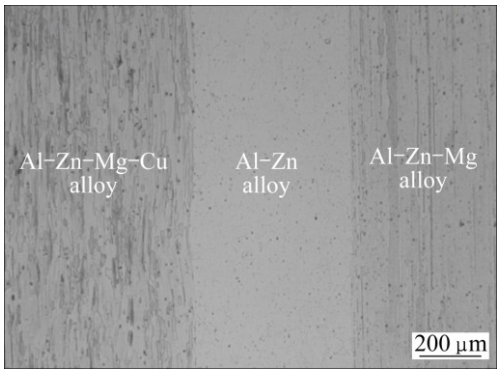

Fig. 1 OM image of 7B52-T6 ALC plate composed of Al−Zn−Mg, Al−Zn and Al−Zn−Mg−Cu alloys

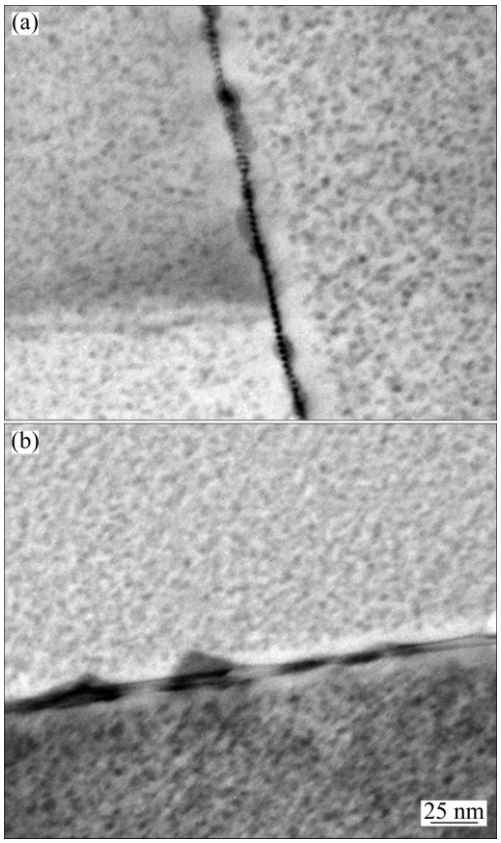

Fig. 2 TEM images of nano-scale particles and grain boundary precipitates in individual layers of Al−Zn−Mg alloy (a) and Al−Zn−Mg−Cu alloy (b) in T6 treatment

in the Al−Zn−Mg−Cu alloy (Fig. 2(b)), indicating that the strength of Al−Zn−Mg−Cu alloy will be higher than that of Al−Zn−Mg alloy. The grain boundary precipitates in the Al−Zn−Mg alloy are small sphere-like and discretely distributed (Fig. 2(a)), while those particles in the Al−Zn−Mg−Cu alloy are coarse rod-like and continuously distributed (Fig. 2(b)). These small sphere-like and discontinuously distributed grain boundary particles are believed to beneficial for the toughness of the Al−Zn−Mg alloy [19], and actually the elongation of the Al−Zn−Mg alloy is higher than that of the Al−Zn−Mg−Cu alloy. The mechanical properties of Al−Zn−Mg and Al−Zn−Mg−Cu alloys in the 7B52 ALC plate are as shown in Table 1. Hence, the 7B52 ALC plate combines the high strength of the Al−Zn−Mg−Cu alloy and the good toughness of the Al−Zn−Mg alloy together, thus, it can perform the excellent ballistic property [16].

Table 1 Mechanical properties of Al−Zn−Mg and Al−Zn−Mg−Cu alloys in 7B52 ALC plate

Alloy	Temper	Ultimate tensile strength/MPa	Yield strength/MPa	Elongation/%
Al−Zn−Mg	T6	≥450	≥350	≥7
Al−Zn−Mg−Cu	T6	≥500	≥430	≥5

3.2 Non-destructive test and mechanical tensile test of bonding interfaces

UFD technology was used to examine the shapes and locations of the defects throughout the bonding interfaces of 7B52 ALC plate, and the flaws could be detected by ultrasonic pulse-echo signals during ultrasonic testing. It is found that the large nummular defects nearly align parallel to the rolling direction at the Al−Zn−Mg−Cu/Al−Zn interface (Fig. 3(a)), but the small defects array irregularly at the Al−Zn/Al−Zn−Mg interface (Fig. 3(b)), indicating that the Al−Zn alloy does not bond well with the Al−Zn−Mg alloy and Al−Zn−Mg−Cu alloy. In order to analyze the formation mechanism of this phenomenon, the samples with 15 mm in diameter and defects (marked by two circles in Figs. 3(a) and (b)) were cut from the 7B52 ALC plate.

The Al−Zn−Mg−Cu/Al−Zn interface and the Al−Zn/Al−Zn−Mg interface were separated during tensile test, and their interfacial tensile strengths of 120 and 180 MPa were measured, respectively. The fracture surfaces of two interfaces are shown in Fig. 4. It is seen that the former with large defect is smooth except for the central dimple fracture (Fig. 4(a)), but the latter with small defect is the ductile fracture except for the unbonding zones (Fig. 4(b)). The fracture surface presents three stages (crack initiation, stable crack growth and final fracture) of the fracture marked by

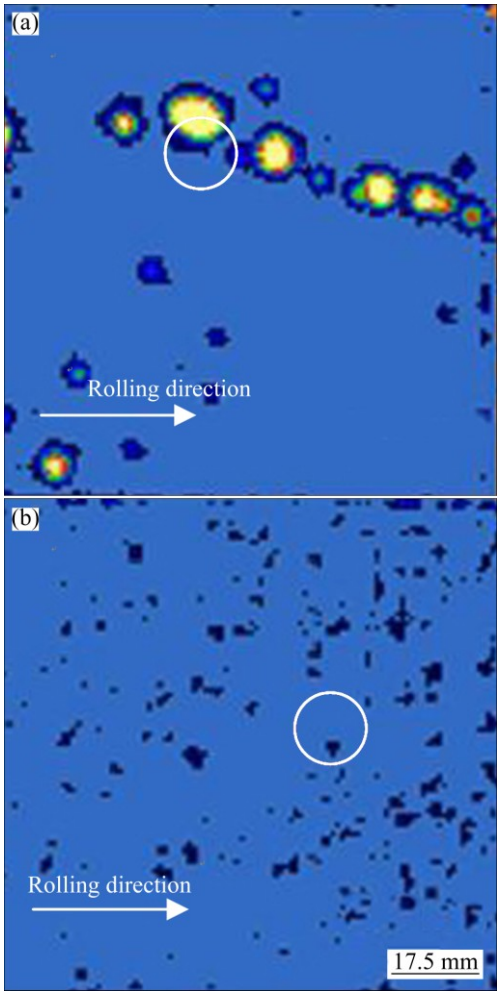

Fig. 3 Ultrasonic flaw detection detecting graphs of Al−Zn−Mg−Cu/Al−Zn interface (a) and Al−Zn/Al−Zn−Mg interface (b)

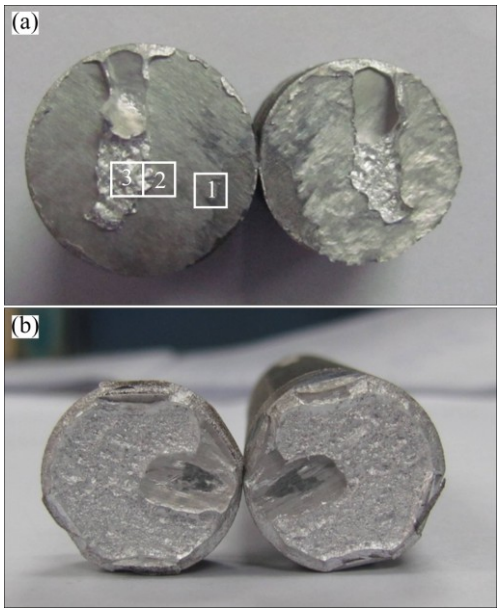

Fig. 4 Photographs of macro-fracture surfaces of Al−Zn−Mg−Cu/Al−Zn interface (a) and Al−Zn/Al−Zn−Mg interface (b) with defects

rectangles in Fig. 4(a). Obviously, this dimple fracture verifies the existence of good metallurgical bonding interface in 7B52-T6 ALC plate. The metallurgical bonding mode induces the failure of the individual Al−Zn layer rather than the fracture of the bonding interface, which also contributes to the high bonding strength of 180 MPa.

3.3 SEM analysis of bonding interfaces with defect

For revealing the formation reason of interface defects, the enlarged fracture areas on the Al−Zn−Mg−Cu/Al−Zn interface were observed. There are dark and light morphologies in the transition zones, which contains the area from crack initiation to crack growth (Fig. 5(a)). At the same time, many impurities distributed in the dark morphology in Figs. 5(a) and (b) show the crack growth zone mostly comprised of light morphology. In Fig. 5(d), it is observed that the failure interface is characterized by tearing ridges. The dimples (Fig. 5(c)) are originated from the ductile fracture process, which indicates that the fracture occurs within the layer of Al−Zn alloy. This result also implies that the bonding strengths of the metallurgical bonding interface free of the defects are higher than that of the Al−Zn alloy. Hence, the dimple fracture confirms that the composite rolling process is advanced.

Figure 6(a) shows the impurities and clusters of constituent particles existed evidently on dark smooth fracture surface. The impurity marked by *A* in Fig. 6(a) was determined as metal oxide with oil. By the EDS analysis, the impurity contains O, Al, Zn and Na (Fig. 6(b)), the clusters marked by *B* in Fig. 6(a) consist of many polyhedral particles containing Al, Zn, Na and Cl, which are deemed to be residues of acid wash (Fig. 6(c)). Moreover, Fig. 6(a) also shows that fracture surface is smooth, and no deformation occurs in the matrix, indicating that the air is sandwiched between two individual layers. These lead to bubble-like defects paralleling to the rolling direction, which is consistent with the observation shown in Fig. 3(a). Figure 6(d) shows the light and dark morphologies of the fracture surface. The light morphology free of the defect is characterized by tearing ridges, and the dark morphology with thick oxide layer is cracked during the rolling process, as shown in the locations marked by the rectangles. There is an obvious crack at the junction of the light and dark morphologies, and clusters of coarse particles located on the boundary of this crack contain Al, Zn, Cu, Mn and Fe detected by EDS (Fig. 6(e)). The analysis of the peak ratios of multiple spectra suggests

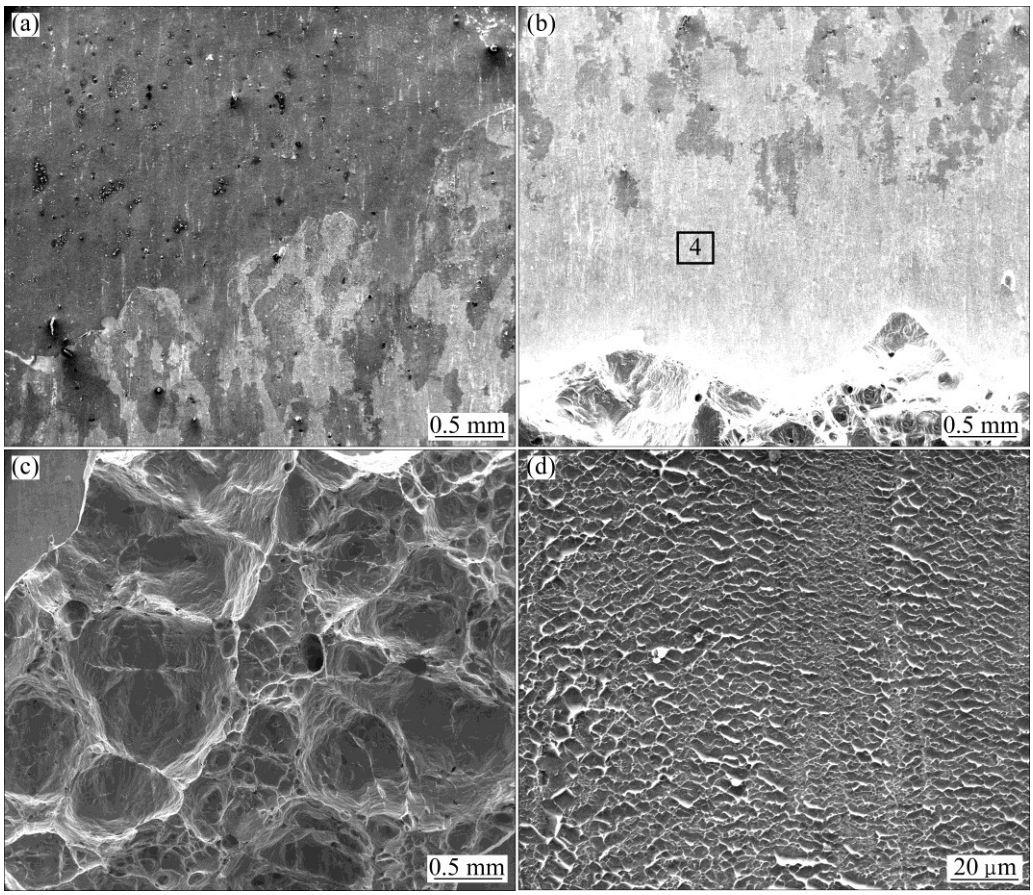

Fig. 5 SEM images of fracture surfaces of Al−Zn−Mg−Cu/Al−Zn interface at rectangles 1(a), 2(b) and 3(c) in Fig. 4(a), and rectangle 4 in Fig. 5(b) (d)

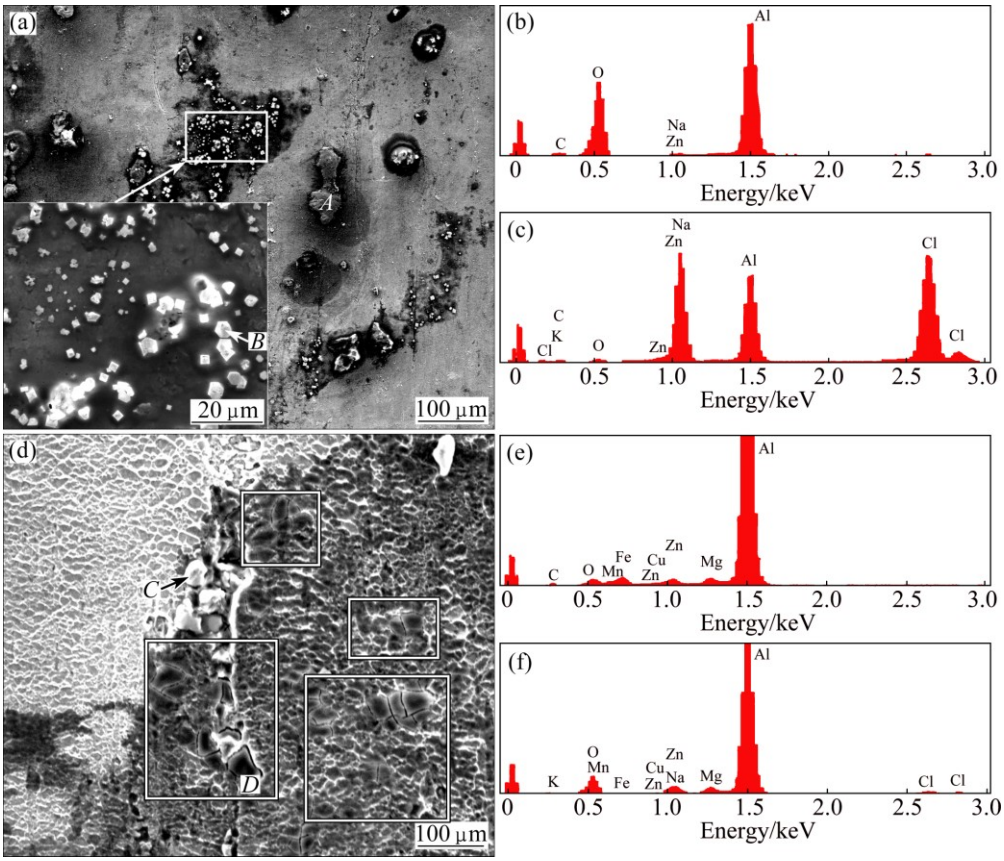

Fig. 6 SEM images of fracture surface of defects on bonding interface (a, d), and EDS spectra of impurities marked by *A* (b) and *B* (c) in Fig. 6(a) and constituent particles marked by *C* (e) and *D* (f) in Fig. 6(d)

that these are coarse constituent phase particles, namely Fe-rich phase (Fig. 6(f)). The presence of metal oxide, oil, air, thick oxide films and coarse particles on the fracture surface suggests that they were not cleaned out during the surface treatment. These defects promote the development of microcracks easily. These reveal that surface treatment technology before composite rolling needs to be further improved, because the surface quality of the individual layers directly affects the bonding state of the interface.

4 Discussion

The deformation and individual layer shapes of 7B52 ALCs are affected by the composition and thickness of the individual layer (Fig. 1). The design and effective control of individual layer's shape play important roles in enhancing the performance of 7B52 ALCs during the rolling bonding process. The previous work [16] shows that the material optimum option of single layer is necessary (as shown in Fig. 2), and compared with the 7A52 single alloy, the 7B52 ALC has the excellent particular performances by the reasonable design of the composition and structure. Under impact, energy is mainly dissipated in the Al−Zn−Mg−Cu layer, and crack expanding is obviously impeded by the Al−Zn layer and the Al−Zn−Mg layer. The non-uniform deformation of component metals can lead to the complex individual layer shapes of ALCs [14]. The complex interface shape affects the mechanical properties of ALCs, and brings great difficulties for the prediction of performance.

Composite rolling process can play an important role in enhancing the interface bonding quality. This process generates extremely large interfacial pressures by large plastic deformation, ultimately causing strong adhesion of the components. The characterizations of composite hot-roll bonding (CHRB) techniques are as follows: 1) the interfaces of composite plates have good bonding quality (Fig. 1); 2) the thickness of composite plates is hard to control, there are poor consistency and stability (defects like bubbles shown in Fig. 3(a)). The CHRB technology in this work is suitable for the production of 7B52 composite plates with the unbent interface, as shown in Fig. 1. During the composite rolling, the bonding must be provided with essential bonding energy. The bonding energy E is expressed as: $E=E_e+E_i-E_n$, where E_e is the dissipating energy, E_i is the bonding energy of metallic bond, and E_n is the internal energy during heating and deformation.

Surface treatment can significantly influence the composite roll bonding quality, as clearly illustrated in Figs. 3(b), 5 and 6. The open literature studies [20] have indicated that the mechanism governing hot roll bonding is the fragmentation of the oxide layer due to the deformation of metal through the fragmented cracks to achieve the intimate contact between nascent metal surfaces. However, it is shown that, in every case, the cracked layer of oxides was detected on the surface of the unbonded area, as marked by the red box in Fig. 6(d). This finding, similar to the reported work [20], indicates that the thick oxide layer leads to the unbonded area. The thick oxide layer is difficult to break, thus impeding the establishment of the close contact between nascent metal surfaces. In addition, large amounts of acid washed residues are found at the interface with the unbonded area (Figs. 5(a) and 6(a)). As a result, the inferior bonding quality and delaminated areas are yielded at the Al−Zn−Mg−Cu/Al−Zn interface (Fig. 4(a)).

In this work, we focused on the interface analysis of 7B52 ALC plate. In order to enhance the bonding quality, the improvement of the surface treatment process and the control of the thickness of the oxide layer at the interface require further exploration. It should be noted that the bonding quality is also affected by many other factors such as materials, thickness of individual layer and CHRB parameters (rolling temperature, reduction, etc).

5 Conclusions

1) 7B52 ALC plate fabricated by composite hot-roll bonding techniques possesses good metallurgical bonding and straight interfaces.

2) The oxide layer on the surface of metal and the surface treatment process can play important roles in affecting the bonding quality. If the thickness of oxide layer on the surface can be well controlled or the present surface treatment process can be reasonable improved, it is possible to further improve the bonding quality.

3) The ultrasonic test results are consistent with the SEM analysis. It is shown that the ultrasonic testing is a quantitative measurement which is capable of assessing the bonding interface of 7B52 ALC plate.

References

[1] MILLER W S, ZHUANG L, BOTTEMA J, WITTEBROOD A J, SMET P D, HASZLER A, VIEREGGE A. Recent development in aluminium alloys for the automotive industry [J]. Materials Science and Engineering A, 2000, 280: 37−49.

[2] SANDERS R E, HOLLINSHEAD P A, SIMIELLI E A. Industrial development of non-heat treatable aluminum alloys [J]. Materials Forum, 2004, 28: 53−64.

[3] ALMAN D E, HAWK J A, PETTY A V, RAWERS J C. Processing intermetallic composites by self-propagating high-temperature synthesis [J]. Journal of the Minerals Metals and Materials Society, 1994, 46: 31−35.

[4] KONIECZNY M. Relations between microstructure and mechanical properties in laminated Ti-intermetallic composites synthesized using Ti and Al foils [J]. Advanced Materials, 2014, 592−593: 728−731.

[5] ZHU B, LIANG W, LI X R. Interfacial microstructure, bonding strength and fracture of magnesium−aluminum laminated composite plates fabricated by direct hot pressing [J]. Materials Science and Engineering A, 2011, 528: 6584−6588.

[6] KONIECZNY M, DZIADON A. Strain behavior of copper-intermetallic layered composite [J]. Materials Science and Engineering A, 2007, 460−461: 238−242.

[7] WANG H, HAN J, DU S, NORTHWOOD D O. Effects of Ni foil thickness on the microstructure and tensile properties of reaction synthesized multilayer composites [J]. Materials Science and Engineering A, 2007, 445−446: 517−525.

[8] LI Xiao-bing, ZU Guo-yin, WANG Ping. Microstructural development and its effects on mechanical properties of Al/Cu laminated composite [J]. Transactions of Nonferrous Metals Society of China, 2015, 25(1): 36−45.

[9] SKORPEN K G, MAULAND E, REISO O, ROVEN H J. Novel method of screw extrusion for fabricating Al/Mg (macro-) composites from aluminum alloy 6063 and magnesium granules [J]. Transactions of Nonferrous Metals Society of China, 2014, 24(12): 3886−3893.

[10] HARACH D J, VECCHIO K S. Microstructure evolution in metal-intermetallic laminate (MIL) composites synthesized by reactive foil sintering in air [J]. Metallurgical and Materials Transactions A, 2001, 32: 1493−1505.

[11] XU L, CUI Y Y, HAO Y L, YANG R. Growth of intermetallic layer in multi-laminated Ti/Al diffusion couples [J]. Materials Science and Engineering A, 2006, 435-436: 638−647.

[12] ZHANG X P, YANG T H, LIU J Q, LUO X F, WANG J T. Mechanical properties of an Al/Mg/Al trilaminated composite fabricated by hot rolling [J]. Journal of Materials and Science, 2010, 45: 3457−3464.

[13] ZHANG X P, CASTAGNE S, YANG T H, GU C F, WANG J T. Entrance analysis of 7075 Al/Mg−Gd−Y−Zr/7075 Al laminated composite prepared by hot rolling and its mechanical properties [J]. Materials and Design, 2011, 32: 1152−1158.

[14] CHEN Z J, WU X, HU H B, CHEN Q Z, LIU Q. Effect of individual layer shape on the mechanical properties of dissimilar Al alloys laminated metal composite sheets [J]. Journal of Materials Engineering and Performance, 2014, 23: 990−1001.

[15] VECCHIO K S. Synthetic multifunctional metallic-intermetallic laminate composites [J]. Journal of the Minerals Metal and Materials Society, 2005, 57: 25−31.

[16] ZHOU G X, QIAO L, WANG Y Q, CHENG X Y, SONG J M, WANG S. The study on damage failure pattern and microstructure analysis of target plate of laminated armor Al-alloy [C]//25th International Symposium on Ballistics. Beijing: China Science and Technology Press, 2010, 17−21: 1540−1546.

[17] LI J, ZHAN X L, CHEN S L, JIN S J. Research on an ultrasonic phased array defect detection system [J]. Journal of Applied Sciences, 2013, 13(8): 1376−1381.

[18] DRINKWATER B, WILCOX P. Ultrasonic arrays for non-destructive evaluation: A review [J]. NDT and E International, 2006, 39(7): 525−541.

[19] DUMONT D, DESCHAMPS A, BRECHET Y. On the relationship between microstructure, strength, and toughness in AA7050 aluminum alloy [J]. Materials Science and Engineering A, 2003, 356: 326−336.

[20] LIU J T, LI M, SHEU S, KARABIN M E, SCHULTZ R W. Macro- and micro-surface engineering to improve hot roll bonding of aluminum plate and sheet [J]. Materials Science and Engineering A, 2008, 479: 45−57.

7B52 叠层铝合金轧制复合界面分析

周古昕，郎玉婧，郝 洁，刘 稳，王 生，乔 丽，陈 敏

中国兵器科学研究院宁波分院，宁波 315103

摘 要：通过金相、透射电镜、扫描电镜、超声无损检测和结合强度测试，研究 7B52 叠层铝合金热轧复合的结合界面。结果表明：轧制复合能够使界面获得冶金结合。TEM 分析和拉伸试验表明：7B52 叠层铝合金板材是由高强度硬层材料和高韧性软层材料复合而成。然而，超声无损检测和 SEM 分析表明：结合界面处的缺陷(如厚氧化层、酸洗残留物、空气、油渍和粗大粒子等)不利于界面结合强度。总之，轧制复合工艺适用于 7B52 叠层铝合金板材，且应该严格控制缺陷的数量和尺寸。先进的单层板表面处理技术有利于进一步提升结合质量。

关键词：7B52 叠层铝合金；轧制复合；显微组织；界面分析

(Edited by Mu-lan QIN)